ANALYTICAL SCIENCES JULY 2018, VOL. 34

2018 © The Japan Society for Analytical Chemistry

Development of Titania Nanotube-based Electrochemical Immunosensor and Determination of Prostate Specific Antigen

Damla KIZILTAN,*1 Tayfun VURAL,*2 Cem BAYRAM,*3 Serhat OZTURK,*2 Betul BOZDOGAN,*4 Yesim Tugce YAMAN,*5 Serdar ABACI,*5 and Emir Baki DENKBAS*1,*2†

*1 *Bioengineering Division, Hacettepe University, Ankara, Turkey*
*2 *Chemistry Department, Biochemistry Division, Hacettepe University, Ankara, Turkey*
*3 *Advanced Technologies Application and Research Center, HUNITEK, Hacettepe University, Ankara, Turkey*
*4 *Nanotechnology and Nanomedicine Division, Hacettepe University, Ankara, Turkey*
*5 *Chemistry Department, Analytical Chemistry Division, Hacettepe University, Ankara, Turkey*

Early diagnosis of cancer is the most important factor that increases the success of treatment. Therefore, the development of new diagnostic tools is a necessity. In this study, a new electrode surface was developed *via* modification of a disposable titanium electrode with anodic oxidation and coating of gold nanoparticle and chitosan. Titanium electrodes were anodized by several anodization parameters to obtain a nanoporous surface and characterized by scanning electron microscopy. Electrodes anodized in optimum conditions were modified with gold nanoparticles and chitosan for enhancing conductivity and functionalizing the surface of electrode, respectively. To detect prostate specific antigen (PSA), anti-PSA was bound onto the functional electrode surface. Modified electrodes were characterized with scanning electron microscopy and cyclic voltammetry and used for chronoamperometric detection of PSA. Limit of detection (LOD) of the designed electrode was found to be 7.8 ng mL^{-1} for PSA in a linear range of 0 – 100 ng mL^{-1}.

Keywords Prostate specific antigen, electrochemical biosensor, titanium electrode, gold nanoparticle, chitosan

(Received August 15, 2017; Accepted February 9, 2018; Published July 10, 2018)

Introduction

The development of effective diagnostic systems has become a rapidly increasing need for new therapy modalities. New strategies based on optical, electrochemical, radiological, piezoelectrical and immunological transduction have been developed for detecting and monitoring of psychochemical properties of an object.[1] Electrochemical biosensors scan electroactive species produced or consumed by the bio-recognition process based on potentiometric, amperometric or impedimetric transduction principles.[2,3] Electrochemical sensors offer various advantages such as high sensitivity, cost effectivity, fast analysis, simple preparation, ease of use, portability, disposability in most cases, small analyte volume, and simple instrumentation. These sensors therefore have a wide range of applications including those related to the environment, food, defense, and especially medicine.[4] The most accelerating development in sensor science is the integration of nanomaterials into sensor fabrication processes. Due to their superior physicochemical properties, they improve the performance of sensors.[5,6]

Cancer is the second cause of disease-related deaths after cardiovascular diseases. According to the report of the World Health Organization in 2014, 14.1 million new cases of cancer were recorded in 2012 and it is expected that this number will reach 25 million in 2030.[7] A large number of cancer-related deaths are attributable to breast cancer in women and prostate cancer in men. According to the research in 2016, while overall cancer incidence trends between 2009 and 2012 were stable in women, the rate declined by 3.1% per year in men due to the spike in detection of prostate cancer as a result of prostate-specific antigen (PSA) monitoring.[8] These results highlight the importance of early detection for the success of cancer treatment.

The working principle of immunosensors is based on the affinity between antigen and antibody. Immunosensors have high specificity and a low limit of detection due to high affinity of the antibody to their antigen.[9,10] The determination of tumor markers at low concentrations is necessary for early diagnosis and therefore this increases the success of cancer treatment as aforementioned. Electrochemical immunosensors are analytical devices for quantitative detection of biomarkers.[11–13] The National Cancer Institute defines a biomarker as "a biological molecule found in blood, other body fluids, or tissues that is a sign of a normal or abnormal process or of a condition or disease. A biomarker may be used to see how well the body responds to a treatment for a disease or condition".[14] Some marker levels are associated with various diseases especially with cancer.[15,16] Prostate-specific antigen (PSA) is a serine protease; its physiological role is believed to be condensing the seminal fluid. Prostate cancer causes the release of PSA into the circulatory system and increases the level in blood up to 10^5-fold. Measuring the blood level of PSA is the most commonly used method in diagnosis of prostate cancer.[17,18] A PSA concentration in blood between 4 – 10 ng mL^{-1} is

† To whom correspondence should be addressed.
E-mail: denkbas@hacettepe.edu.tr

considered a "gray zone" for prostate cancer, while a PSA concentration above 10 ng mL^{-1} indicates prostate cancer.[19,20]

The aim of the present research is to develop an electrochemical immunosensor based titanium electrode modified by nanotechnology. For this purpose, titanium alloyed electrodes were subjected to anodic oxidation for forming of a titanium oxide (titania) tubular structure on the electrode surfaces. An electrode with high surface area promotes more efficient electron transfer.[21] After forming nanotubes, the titania electrode surface was coated with chitosan and gold nanoparticles. Chitosan provides functionalization of the electrode surface with reactive amine functional groups for binding of PSA and an immobilization matrix for gold nanoparticles. Gold nanoparticles are used in electrochemical studies because of their high surface area and synergistic effect with several materials. Several approaches have appeared in the literature where the ability of AuNPs to enhance electrocatalytic activity, the electron transfer rate, and conductivity have been presented.[22,23] For this purpose, AuNPs can be found in a polymer or on an electrode surface.[24-26] Following the coating with chitosan and AuNPs, anti-PSA as recognizing molecule was placed on the electrode surface for detection of PSA. The designed biosensor hold promise for early cancer diagnosis.

Experimental

Reagents and chemicals

Titanium wires (d: 0.25 mm, 99.5% purity, Alfa Aesar, USA), ethylene glycol (Merck, Germany), ammonium fluoride (NH_4F, Sigma-Aldrich, ABD), phosphoric acid (H_3PO_4, 85% purity, Merck, Germany), nitric acid (HNO_3, 65% purity Merck, Germany), hydrofluoric acid (HF, 38% purity, Merck, Germany) and 2×2 cm pure platinum mesh (99.9% purity; 0.1 mm thickness, Alfa Easer, USA) as an anodic oxidation opposing electrode were used to produce anodized titanium electrode.

For electrode modification, hydrogen tetrachloroaurate ($HAuCl_4$, Sigma, USA), phosphate buffer solution (PBS) tablet (10 mM, pH 7.4, Alfa Aesar, England), PSA-protein (Fitzgerald, USA), PSA-antibody (Fitzgerald, USA), PSA-antibody-HRP (Fitzgerald, USA), 1-ethyl-3-(3-dimethylaminopropyl)carbodiimide (EDC, Sigma, USA), *n*-hidroxysuccinimide (NHS, Sigma, USA), Tween-20 (Sigma, USA), bovine serum albumin (BSA, Sigma, USA), acetic acid (Sigma, USA), low molecular weight chitosan (Sigma, USA), isopropyl alcohol (Merck, Germany), hydrogen peroxide (30% purity, Merck, Germany), and hydroquinone (Kanto, Singapore) were used. All liquid solutions contained deionized (DI) water with a resistance of 18.2 MΩ·cm.

Apparatus

Morphology of electrodes was characterized with Zeiss Evo 60 scanning electron microscopy (SEM). All electrochemical measurements were carried out using CH Instrument Potentiostat/Galvanostat in a three-electrode configuration. The modified electrode was used as the working electrode by dipping 1 cm of the electrode in a three-electrode cell. Reference electrode was Ag/AgCl (3.0 M KCl) and counter electrode was platinum wire. Before measurements, all solutions were deaerated with pure nitrogen gas for about 20 min. Ultraviolet-visible (UV-Vis) absorbance spectrum and particle size distribution of the synthesized colloidal gold nanoparticles were obtained by using UV-Vis absorbance spectrophotometer (Thermo, 1000 Nanodrop, USA) and dynamic light scattering analyzer (Malvern, Zetasizer Nano ZS, UK), respectively.

Procedures

Anodization of titanium electrodes. Titanium wires were cleaned with diluted detergent and deionized water for about 5 min, then in 70% ethyl alcohol solution, in ultrasonic bath for 20 min. Finally, the titanium wires were left for 10 min in a solution containing 1% HF and 1.5% HNO_3 to remove the unstable and inactive oxide layer on their surfaces and then rinsed with deionized water.

The cleaned titanium wires were anodized in order to obtain a nanoporous surface with high surface area similar to the method in the literature.[27] For this purpose, the titanium wires placed in the appropriate electrolyte solution were connected to the platinum mesh, which were also immersed in the same solution, so that power from the power source would reach the titanium wires from the positive terminal, and voltage was applied at different levels. In the anodization process, an electrolyte solution containing 0.5% H_3PO_4 and 0.2 M NH_4F, with a 50% water and ethylene glycol mixture, was used. The duration of the anodization process was 15 – 60 min. With time being the non-variable measurement, the treated wires were anodized at 20, 30, 40, 50, and 60 V potential differences. Distance between the electrodes was 3 cm in the anodization process. Lastly, the anodized titanium electrodes were sintered at 450°C for 90 min. The resulting electrodes were denoted as AnTi.

Modification of AnTi electrodes by controlled potential coulometry in $HAuCl_4$ solution. AnTi electrode, as working electrode in a three electrode system, was dipped in a 0.5 mg mL^{-1} $HAuCl_4$ solution (prepared with 0.5 M H_2SO_4) and gold nanoparticles (AuNPs) were formed on the anodized electrode surface by controlled potential coulometry at –0.3 V *vs.* Ag/AgCl for 120 s.[28] The resulting electrode was denoted as AuNP/AnTi.

Synthesis of colloidal gold nanoparticles. The citrate-stabilized AuNPs were prepared according to the reported procedure with minor modifications.[29] First, 40 mg of gold(III) chloride trihydrate ($HAuCl_4 \cdot 3H_2O$) was dissolved in 100 mL DI (deionized) water for the synthesis of gold nanoparticles. It was then heated until its boiling temperature was reached while stirring with a heated magnetic stirrer at 1000 rpm. Next, 120 mg of trisodium citrate dihydrate ($C_6H_5Na_3O_7 \cdot 2H_2O$) dissolved in 10 mL DI water was added. It was boiled for 1 h and turned into a dark red color and was then allowed to cool at room temperature and stored at +4°C.

Modification with gold nanoparticle–chitosan (AuNP–CH). Chitosan (CH), which is a natural biopolymer, was used as a matrix for immobilization of anti-PSA onto the electrode surface. The AuNP–CH composite was prepared by mixing AuNP solution with CH solution. Final solution included 0.145 mg mL^{-1} AuNP in CH solution with three different concentrations (0.1, 0.5, and 1.0%). AuNP/AnTi electrodes were modified with AuNP–CH using two different methods according to the predescribed method in the literature with minimal modification.[30,31] In the first method, the electrodes were incubated into the AuNP–CH solution and after 15 min of waiting, they were removed and immersed in 0.1 M NaOH solution, after which they were washed with DI water and dried at room temperature.[30] Chitosan, which is an amine rich polysaccharide, has been used as an immobilization matrix to stabilize the metal nanoparticles due to its high metal affinity.[32-34] Chitosan was adsorbed on the titanium surface by physical adsorption *via* electrostatic or van der Waals interactions between the positively charged amine groups of chitosan and oxide layer of AnTi electrode (TiO^-).[35,36] In the second method, the electrodes were modified by constant potential electrolysis for 5 min at 3.0 V *vs.* Ag/AgCl in the AuNP–CH solution. By electrolysis, hydroxide ions were generated as a result of the

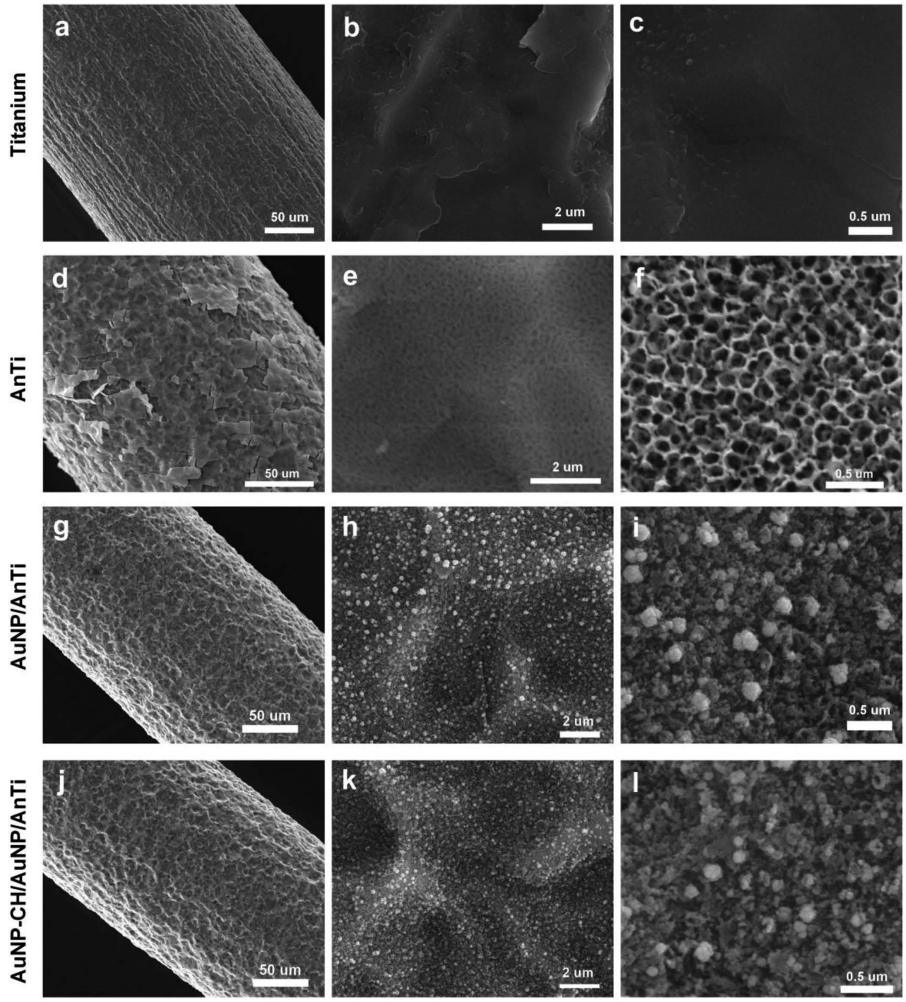

Fig. 1 SEM images of Ti electrode (a – c), AnTi electrode (d – f), AuNP/AnTi electrode (g – i), and AuNP-CH/AuNP/AnTi electrode (j – l).

reduction of water at the surface of the electrode. Then protonated chitosan was neutralized and formed a film on the surface of the electrode.[31] The resulting electrodes were denoted as AuNP-CH/AuNP/AnTi.

Fabrication of immunosensor electrodes. To fabricate the immunosensor, anti-PSA (Ab1) was attached to the AuNP-CH/AuNP/AnTi electrode surface. For this purpose, 0.2 mM EDC was dissolved in PBS and then Ab1 was added to a final concentration at 10 μg mL^{-1}. The NHS (0.4 mM) was added into the Ab1 and EDC solution. The solution was left at room temperature for 10 min for activation of carboxylic acid functional groups of Ab1. Electrodes were then immersed in the solution for 1 h to bind Ab1 to the electrode surface. After 1 h, the electrodes were immersed in washing solution (0.05% tween-20 in PBS) for 5 min, and then in the PBS solution for another 5 min.

To prevent non-specific binding of the electrodes to PSA, the electrodes were interacted with bovine serum albumin (BSA). For this purpose, Ab1/AuNP-CH/AuNP/AnTi electrodes were left for 1 h in a 2% (w/w) BSA solution which was prepared with the washing solution. Electrodes removed from the solution were kept in the washing solution for 5 min and in PBS for another 5 min.

The Ab1/AuNP-CH/AuNP/AnTi electrodes were incubated for 1 h in PSA (Ag) solutions at different concentrations prepared with PBS. After 1 h, the electrodes were washed in the washing solution for 5 min, then in the PBS solution for another 5 min.

Horseradish peroxidase (HRP) attached anti-PSA (HRP-Ab2) was bound to the Ag/Ab1/AuNP-CH/AuNP/AnTi electrodes. The HRP-Ab2 solution was prepared to have a concentration of 0.2 μg mL^{-1} in PBS and the electrodes were left in this solution for 1 h. After 1 h, the electrodes were washed in the washing solution for 5 min, then in the PBS solution for another 5 min. The electrodes were then stored at +4°C in PBS for use in further experiments. The resulting electrode was denoted as Ab2/Ag/Ab1/AuNP-CH/AuNP/AnTi.

Results and Discussion

Morphological characterization of electrodes

Scanning electron microscopy (SEM) was used to evaluate the effect of the anodization time and the applied voltage to the surface morphology of AnTi electrodes. According to the SEM images, a nanoporous, ordered, and homogeneous electrode surface was achieved with anodization at 50 V for 15 min (Figs. S1 and S2, Supporting Information). These electrodes were used in the subsequent experiments. The effects of anodization and modification with AuNPs and AuNP-CH on the

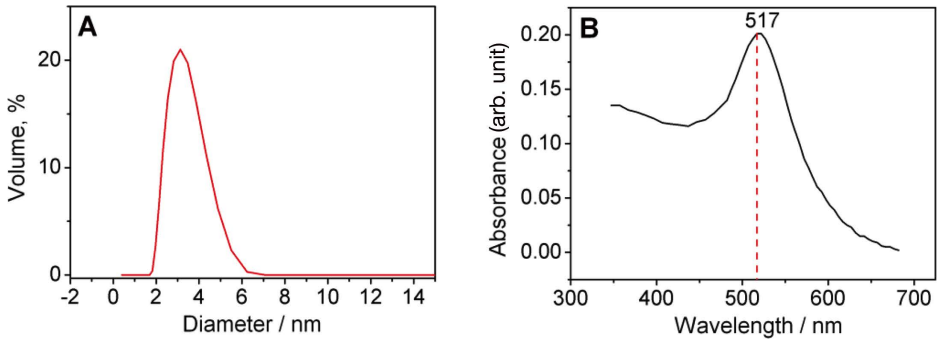

Fig. 2 (A) Size distribution graph and (B) UV-Vis absorbance spectrum of synthesized gold nanoparticles.

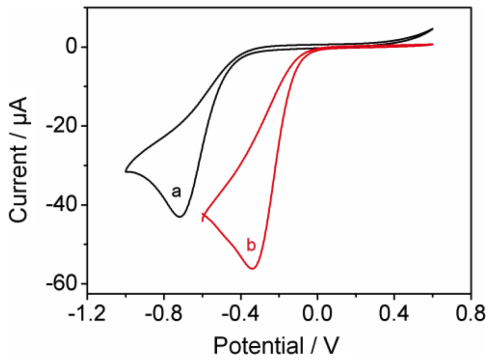

Fig. 3 Cyclic voltammograms of (a) AnTi and (b) AuNP/AnTi electrode in 5 mM $Fe(CN)_6^{3-}$ including 0.1 M KCl (scan rate: 100 mV s^{-1}).

surface morphology of titanium (Ti) electrodes are presented in Fig. 1. A non-anodized and unmodified Ti electrode is shown in Figs. 1a – 1c at different magnifications. After anodic oxidation, titania nanotubes formed on the surface of the Ti electrode (Figs. 1d – 1f). The electrochemical deposition of AuNPs on the titania electrode was confirmed by SEM analysis (Fig. 1g – 1i). Accordingly, formation of AuNP aggregates with different diameters (10 – 200 nm) were displayed on the AnTi surface. Likewise, images of the modified surface of AuNP/AnTi with AuNP-CH are presented in Figs. 1j – 1l. It was concluded that AuNP-CH thin-film was formed on the AuNP/AnTi electrode.

Physicochemical characterization of colloidal gold nanoparticles

Size distribution of the colloidal nanoparticles was found to be about 3.0 nm with dynamic light scattering analyzer (Fig. 2A). Also, absorbance wavelength of gold nanoparticles was 517 nm, which is consistent with the literature (Fig. 2B).[37]

Voltammetric characterization of anodized and modified electrodes

Anodized titanium (AnTi) and AuNP/AnTi electrodes were characterized by cyclic voltammetry in 5 mM $Fe(CN)_6^{3-}$ including 0.1 M KCl. According to Fig. 3, AuNP modification of the AnTi electrode shows electro-catalytic activity and more positive reduction potential for Fe^{III} due to nanosized gold nanoparticle and nanotubular structure of titania that provide a high surface area for more efficient electron transfer.[21,38]

Then, dipping and electrolysis methods were used for gold nanoparticle-chitosan modification of AuNP/AnTi electrode. Comparison of voltammograms of modified electrodes in 5 mM $Fe(CN)_6^{3-/4-}$ including 0.1 M KCl is shown in Fig. 4.

According to Fig. 4, the highest oxidation/reduction peak current was obtained by using 0.1% chitosan solution. Also, the electrolysis method exhibited a higher peak current compared to the dipping method, so it is concluded that chitosan film formation is more controllable by electrolysis than dipping. Therefore AuNP-CH modification was carried out by electrolysis at a concentration of 0.1% CH solution for further experiments.

Chronoamperometric detection of PSA

Detection of PSA was carried out by chronoamperometry. A prepared HRP-Ab2/Ag/Ab1/AuNP-CH/AuNP/AnTi electrode was used as the working electrode to determine PSA. Reactions that occurred on the electrode surface are as follows.[39]

$$H_2O_2 + HRP_{red} \rightleftharpoons H_2O + HRP_{ox} \quad (1)$$

$$HRP_{ox} + HQ \rightleftharpoons HRP_{red} + BQ \quad (2)$$

$$BQ + 2e^- + 2H^+ \rightleftharpoons HQ \quad (3)$$

First, HRP catalyzes reduction of H_2O_2 to H_2O. Then oxidation of HQ to benzoquinone (BQ) occurs while HRP_{ox} is regenerated to HRP_{red}. Lastly, BQ is reduced to HQ and causes an increase in the current.

Cyclic voltammetry of the modified electrode was carried out with 0 ng mL^{-1} PSA and 25 ng mL^{-1} PSA in PBS containing 1.0 mM HQ and 1.0 mM H_2O_2 to determine the working potential of the electrode for chronoamperometric detection (Fig. 5). HQ was used as a mediator for electron transportation from enzyme to electrode surface. According to Fig. 5, oxidation peak potential of hydroquinone is at approximately –0.65 V. Therefore, chronoamperometric experiments were performed at –0.65 V with varying concentrations of PSA (Fig. 6). Steady state current values were recorded after 120 s and the calibration graph was plotted. The regression equation was obtained as;

$$I\ (\mu A) = 0.421C\ (\text{ng mL}^{-1}) + 19.3$$

Limit of detection was 7.8 ng mL^{-1} for PSA, calculated according to the $3s/m$ criteria where m is the slope of the calibration graph and s is the standard deviation of three amperometric signals obtained without target PSA.

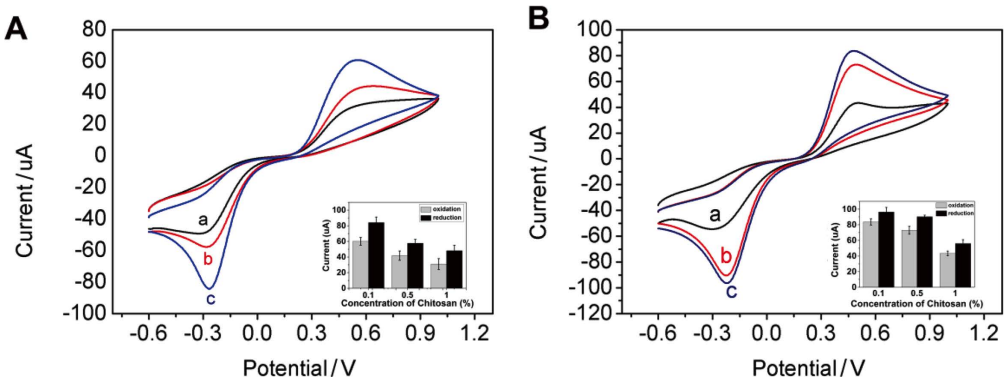

Fig. 4 Cyclic voltammograms of AuNP/AnTi electrode modified with AuNP–CH including a) 1.0% chitosan, b) 0.5% chitosan, and c) 0.1% chitosan by dipping (A) and electrolysis (B) methods (in 5 mM $Fe(CN)_6^{3-/4-}$ including 0.1 M KCl, scan rate: 100 mV s^{-1}) (inset: oxidation and reduction currents of $Fe(CN)_6^{3-/4-}$).

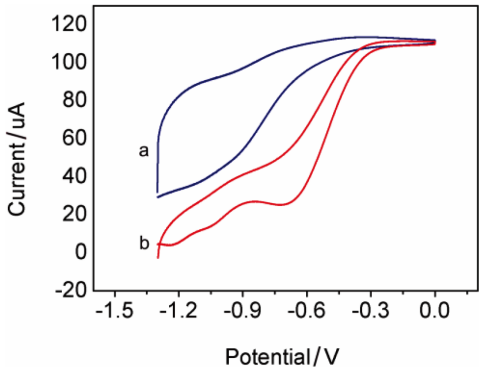

Fig. 5 Cyclic voltammograms of HRP-Ab2/Ag/Ab1/AuNP-CH/AuNP/AnTi electrodes with a) 0 ng mL^{-1} PSA and b) 25 ng mL^{-1} PSA in PBS containing 1.0 mM HQ and 1.0 mM H_2O_2 (pH: 7.4, scan rate: 100 mV s^{-1}).

Conclusions

In summary, the presented work describes a nanotechnological approach to modification of titanium electrodes for enhancing their conductive properties. Electrochemical characterizations confirmed that etching of electrodes by anodization and coating of the surface with gold nanoparticles enhance the sensitivity of the electrode by lowering the limit of detection. The sensitivity of the electrode is very important for early diagnosis of the diseases. The novel modified titanium electrode was used as an immunosensor in cancer diagnosis in the literature for the first time. The developed immunosensor has the potential to be used for the early detection of many diseases and promises for future applications.

Supporting Information

SEM images of the titanium electrodes anodized with different potentials and times are shown. This material is available free of charge on the Web at http://www.jsac.or.jp/analsci/.

References

1. S. Song, H. Xu, and C. Fan, *Int. J. Nanomed.*, **2006**, *1*, 433.
2. J. L. Hammond, N. Formisano, P. Estrela, S. Carrara, and J. Tkac, *Essays Biochem.*, **2016**, *60*, 69.
3. D. Grieshaber, R. MacKenzie, J. Vörös, and E. Reimhult, *Sensors*, **2008**, *8*, 1400.
4. C. I. L. Justino, A. C. Duarte, and T. A. P. Rocha-Santos, *TrAC, Trends Anal. Chem.*, **2016**, *85*, 36.
5. M. Holzinger, A. Le Goff, and S. Cosnier, *Front. Chem.*, **2014**, *2*, 63.
6. M. Hasanzadeh and N. Shadjou, *TrAC, Trends Anal. Chem.*, **2016**, *80*, 167.
7. World Health Organization (WHO), World Health Statistics 2014, **2014**.
8. R. L. Siegel, K. D. Miller, and A. Jemal, *Ca-Cancer J. Clin.*, **2016**, *66*, 7.
9. E. Burcu Bahadır and M. Kemal Sezgintürk, *Talanta*, **2015**, *132*, 162.
10. V. S. P. K. S. A. Jayanthi, A. B. Das, and U. Saxena, *Biosens. Bioelectron.*, **2017**, *91*, 15.
11. J. Lin, W. Qu, and S. Zhang, *Anal. Sci.*, **2007**, *23*, 1059.
12. Y. Zhang, R. Chen, L. Xu, Y. Ning, S. Xie, and G.-J. Zhang, *Anal. Sci.*, **2015**, *31*, 73.
13. H. C. Yoon, H. Yang, and S. Y. Byun, *Anal. Sci.*, **2004**, *20*, 1249.
14. National Helath Organization, Definition of Biomarker.
15. J. Wu, Z. Fu, F. Yan, and H. Ju, *TrAC, Trends Anal. Chem.*, **2007**, *26*, 679.
16. X. Wang, J. Miao, Q. Xia, K. Yang, X. Huang, W. Zhao, and J. Shen, *Electrochim. Acta*, **2013**, *112*, 473.
17. H. Lilja, D. Ulmert, and A. J. Vickers, *Nat. Rev. Cancer*, **2008**, *8*, 268.
18. T. J. Wilt, P. T. Scardino, S. V Carlsson, and E. Basch, *JNCI, J. Natl. Cancer Inst.*, **2014**, *106*, dju010.
19. K. Yoshida, M. Honda, S. Sumi, K. Arai, S. Suzuki, and S. Kitahara, *Clin. Chim. Acta*, **1999**, *280*, 195.
20. P. Tang, W. Du, K. Xie, X. Deng, J. Fu, H. Chen, and W. Yang, *Urol. Oncol. Semin. Orig. Invest.*, **2013**, *31*, 744.
21. P. Roy, S. Berger, and P. Schmuki, *Angew. Chem., Int. Ed.*, **2011**, *50*, 2904.
22. Y. Ma, X.-L. Shen, Q. Zeng, and L.-S. Wang, *Microchim. Acta*, **2017**, *184*, 4469.

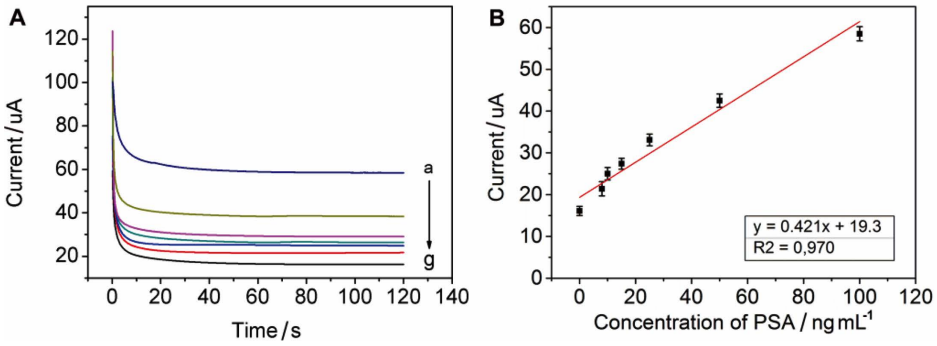

Fig. 6 (A) Chronoamperomograms of HRP-Ab2/Ag/Ab1/AuNP-CH/AuNP/AnTi in 1.0 mM HQ, 0.1 mM H_2O_2 and 10 mM PBS at pH 7.4 for various concentrations of PSA (a) 100, b) 50, c) 25, d) 15, e) 10, f) 8, and g) 0 ng mL^{-1}) at an applied potential of –0.65 V *vs.* Ag/AgCl (scan rate: 0.1 V). (B) Linear calibration curve of current values from chronoamperogram of PSA (0 – 100 ng mL^{-1} PSA).

23. S. Li, Q. Luo, Y. Liu, Z. Zhang, G. Shen, H. Wu, A. Chen, X. Liu, and A. Zhang, *Polymers*, **2017**, *9*, 359.
24. S. A. Kumar, S.-F. Wang, and Y.-T. Chang, *Thin Solid Films*, **2010**, *518*, 5832.
25. E. Yilmaz and S. Suzer, *Appl. Surf. Sci.*, **2010**, *256*, 6630.
26. R.-C. Zhang, D. Sun, R. Zhang, W.-F. Lin, M. Macias-Montero, J. Patel, S. Askari, C. McDonald, D. Mariotti, and P. Maguire, *Sci. Rep.*, **2017**, *7*, 46682.
27. N. Çalışkan, C. Bayram, E. Erdal, Z. Karahaliloğlu, and E. B. Denkbaş, *Mater. Sci. Eng., C*, **2014**, *35*, 100.
28. X. Dai and R. G. Compton, *Anal. Sci.*, **2006**, *22*, 567.
29. I. Nukatsuka, S. Osanai, and K. Ohzeki, *Anal. Sci.*, **2008**, *24*, 267.
30. Y. Li, Y. Zhou, H. Xian, L. Wang, and J. Huo, *Anal. Sci.*, **2011**, *27*, 1223.
31. J. Redepenning, G. Venkataraman, J. Chen, and N. Stafford, *J. Biomed. Mater. Res. Part A*, **2003**, *66A*, 411.
32. H. Huang and X. Yang, *Colloids Surf., A*, **2003**, *226*, 77.
33. Q. Xu, C. Mao, N.-N. Liu, J.-J. Zhu, and J. Sheng, *Biosens. Bioelectron.*, **2006**, *22*, 768.
34. H. N. Kamaruddin, A. A. A. Bakar, N. N. Mobarak, D. M. S. Zan, and N. Arsad, *Sensors*, **2017**, *17*, 2217.
35. Y. Li, B. Li, X. Fu, J. Li, C. Li, H. Li, H. Li, C. Liang, H. Wang, L. Zhou, and S. Xin, *J. Hard Tissue Biol.*, **2013**, *22*, 351.
36. Z. Zhang, T. Jiang, K. Ma, X. Cai, Y. Zhou, and Y. Wang, *J. Mater. Chem.*, **2011**, *21*, 7705.
37. W. Haiss, N. T. K. Thanh, J. Aveyard, and D. G. Fernig, *Anal. Chem.*, **2007**, *79*, 4215.
38. C. Liu, Y. Teng, R. Liu, S. Luo, Y. Tang, L. Chen, and Q. Cai, *Carbon*, **2011**, *49*, 5312.
39. A. J. S. Ahammad, *Biosens. Bioelectron.*, **2013**, *9*, 1.